

Motivation & Background

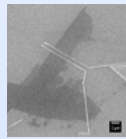
Conventional Junctions



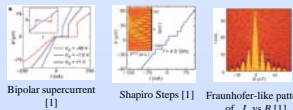
10 μm

A typical niobium/aluminum oxide/niobium SIS junction from Hyplex.

Graphene Junctions

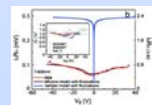


Drexel graphene junction, using 10/70 nm Ti/Al leads separated by $L=200$ nm, with width $W=2.2$ μm

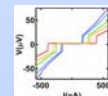


Bipolar supercurrent [1], Shapiro Steps [1], Fraunhofer-like pattern of I_c vs. B [1]

It was found up to date, that these devices are diffusive rather than ballistic by Du et al [3] in 2008.

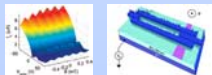


Miao et al [4] found that these devices are underdamped junctions with suppressed critical currents and have strong gate voltage dependence on $I_c R_N$ due to premature switching at ~ 300 mK. (2009)



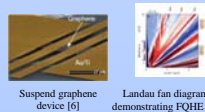
Back gate dependence on L_c and L_R . [4]

Girit et al [5] demonstrated a tunable graphene-based d.c. SQUID (2009).



D.C. SQUID [5]

The fractional quantum Hall effect (FQHE) was recently demonstrated in *suspended* single layer graphene by Du et al [6] and Bolotin et al [7] (2009).



Suspend graphene device [6] Landau fan diagram demonstrating FQHE [7]

It is natural to investigate the existence of macroscopic quantum states in ballistic graphene-based Josephson junctions.

- These graphene devices are attractive because the critical current is tunable via an applied gate voltage, providing an additional knob for quantum control
- Due to straightforward e-beam lithography techniques, devices can be fabricated fairly easily. Multi-junction circuits is a simple next step.
- It is a fruitful and interesting opportunity to study quantum mechanics in a relativistic system.

Acknowledgements

We acknowledge generous help and support from:

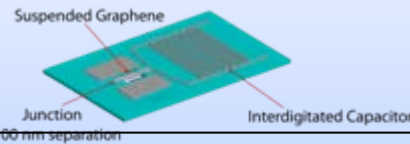
- Prof. Yuri Gogotsi, Min Heon (Drexel Nanomaterials Group) for providing high-quality graphite
- Prof. Jonathan Spanier, grad student Eric Gallo (Drexel Mesomaterials group) for help with fabrication
- Dr. Zhorro Nikolov, for help with Raman spectroscopy
- Prof. Xiaoxing Xi and Prof. Ke Chen (Temple University) for providing high-quality MgB₂ Josephson junction thin films

Abstract

Recently, superconducting tunneling currents have been measured in graphene devices consisting of two parallel superconducting leads contacted by single- and few-layer graphene flakes. The current-voltage characteristic curves of these devices are hysteretic and Shapiro steps appear when the device is irradiated with microwaves. Thus, there is evidence of both the d.c. and a.c. Josephson effects. The graphene devices have shown to have strong quantum coherence as indicated by a Fraunhofer-like pattern in the current versus external magnetic field plot. These effects motivate us to investigate the presence of quantum metastable states similar to those found in conventional current-biased Josephson junctions. We present work investigating the nature of these metastable states and the implications of ballistic versus diffusive graphene Josephson junctions. We also present experimental progress studying the nature of switching from the superconducting to the normal state in these devices.

Proposed Device

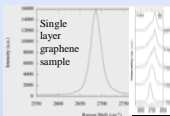
We propose devices consisting of suspended graphene and a parallel on-chip capacitor



- When graphene is suspended, it exhibits the highest level of ballistic transport, such as was used in recent measurements of the FQHE. The ballistic nature is necessary to preserve the quantum phase coherence and to reduce the noise caused by the SiO₂ to resolve quantum states.
- The intrinsic capacitance of the parallel leads is small, $\sim 10^{-16}$ F. Using a typical critical current of ~ 400 nA, equation (3) gives $f_p = \omega_p/2\pi \approx 600$ GHz, in agreement with experimental results.[4,6]
- To lower this frequency to the microwave range which is accessible in our lab, we add a 0.1pF shunting capacitor in an interdigitated design. This reduces the plasma frequency to an experimentally accessible value of $f_p \approx 5$ GHz.

Experimental Progress

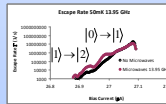
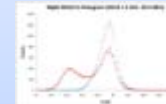
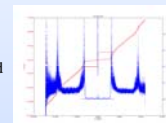
We have produced graphene flakes using the method of mechanical exfoliation [8] and deposited them on n-doped Si/SiO₂ substrates.



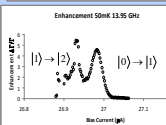
Characterizing Graphene Flakes

- Using Raman spectroscopy, we have confirmed that we have produced single layer graphene [9].
- We produced devices using only optical identification, to avoid potential defects caused by the Raman laser.

We have performed transport and spectroscopy experiments on MgB₂/MgO/Pb junction devices

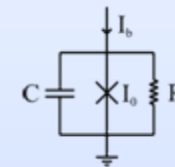


We have seen multiple quantum energy levels in Nb-based current biased Josephson phase qubits [13].

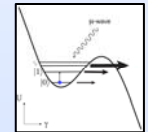


- We deposit Ti/Al (10/70 nm) leads via e-beam lithography and lift off. The Ti provides adhesion, and the Al becomes superconducting below 1K.
- The graphene adjacent to the leads becomes superconducting due to the proximity effect [10].
- A gate voltage is capacitively-coupled to the graphene flake by attaching a wire to the n-doped Si side of the substrate. This presents another way of tuning the quantum device.

Metastable Quantum States



RCSJ Model



The Tilted Washboard Potential

- The current-phase relationship and resultant potential from the Resistively and Capacitively Shunted Junction model in conventional SIS Josephson junctions are [11]

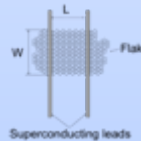
$$I = I_0 \sin \gamma \quad U(\gamma) = -\frac{\Phi_0}{2\pi} (I_0 \cos(\gamma) + I_c \gamma) \quad (1) (2)$$

where γ is the gauge invariant phase difference. The plasma frequency is

$$\omega_p = \sqrt{\frac{2e I_0}{\Phi_0 C}} \left(1 - \left(\frac{I_c}{I_0} \right)^2 \right)^{1/4} \approx \sqrt{\frac{I_0}{C}} \quad (3)$$



- For thin and wide ballistic graphene junctions, $L \ll W$, ξ , the current-phase relationship, critical current, and $I_c R_N$ product at the Dirac point were calculated by Titov and Beenaker [12].



$$I(\phi) = \frac{e \Delta_0 2W}{\hbar \pi L} \cos(\phi/2) \operatorname{arctanh} |\sin(\phi/2)| \quad (4)$$

$$I_0 = 1.33 \frac{e \Delta_0 W}{\hbar \pi L} \quad I_0 R_N = 2.08 \frac{\Delta_0}{e} \quad (5) (6)$$

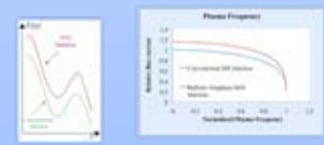
- From this, we calculate the *effective* washboard potential and classical plasma frequency for ballistic graphene junctions

$$U(\gamma) = -\frac{\Phi_0}{2\pi} \left(-\frac{2I_0}{1.33} \left[2 \sin \left(\frac{\gamma}{2} \right) \operatorname{arctanh} \left(\sin \left(\frac{\gamma}{2} \right) \right) \right] + \ln \left(1 - \sin^2 \left(\frac{\gamma}{2} \right) \right) + I_c \gamma \right) \quad (7)$$

$$\omega_p = \left(\frac{2e I_0}{1.33 \Phi_0 C} \right)^{1/2} \left[1 - \sin^2 \left(\frac{\gamma_{min}}{2} \right) \right] \operatorname{tanh}^{-1} \left(\sin \left(\frac{\gamma_{min}}{2} \right) \right)^{1/2} \quad (8)$$

where γ_{min} is the local minimum.

Comparison of washboard potentials and frequency vs. current plots for current-biased conventional and ballistic graphene junctions



Preprint found at arXiv:0908.0713

References

- Heersche et al., Nature 446, 56-59 (2007).
- A. Shailos, W. Nativel, A. Kaimowitz, C. Collet, M. Ferrier, S. Guéron, R. Deblock, and H. Bouchiat, EPL, 79, 57008 (2007).
- Xu Du, I. Skachko, and E. Andrei, Phys. Rev. B 77(18):184507 (2008)
- F. Miao, W. Bao, B. Zhang, and C. N. Lau, Solid State Comm. 149, 1046 (2009)
- Caplar Gier, V. Bouchiat, O. Nannan, Y. Zhang, M. F. Crommie, A. Zettl, and I. Siddiqui, Nano Letters 9,198 (2009)
- Xu Du, I. Skachko, F. Duerr, A. Lucas, and E. Andrei, Nature 462, 192-195 (2009)
- Kiril I. Bolotin, F. Chhabri, M. D. Shuman, H. Stormer, and P. Kim, Nature 462, 196-199 (2009)
- R. S. Novoselov et al., Science 306, 666 (2004).
- A. C. Ferrari et al., PRL 97, 187401 (2006).
- Michael, Tinkham, Introduction to superconductivity, McGraw-Hill, New York, 1975.
- J. M. Martinis, H. Devoret, and John Clarke, Phys. Rev. B 15, 4682 (1987).
- M. Titov and C. W. J. Beenaker, Phys. Rev. B 74, 041401(R) (2006).
- R. C. Ramos, M.A. Gabard, A.J. Berkley, J.R. Anderson, C.J. Lobb, and F.C. Wellstood, IEEE Trans. Appl. Supercon. 11, 998-1001 (2001).